

Realizations of Indecomposable Persistence Modules of Arbitrarily Large Dimension

Mickaël Buchet
TU Graz

Emerson G. Escolar
RIKEN AIP

March 16, 2022

Abstract

While persistent homology has taken strides towards becoming a widespread tool for data analysis, multidimensional persistence has proven more difficult to apply. One reason is the serious drawback of no longer having a concise and complete descriptor analogous to the persistence diagrams of the former. We propose a simple algebraic construction to illustrate the existence of infinite families of indecomposable persistence modules over regular grids of sufficient size. On top of providing a constructive proof of representation infinite type, we also provide realizations by topological spaces and Vietoris-Rips filtrations, showing that they can actually appear in real data and are not the product of degeneracies.

1 Introduction

Recently, persistent homology [9] has been established as a flagship tool of topological data analysis. It provides the persistence diagrams, an easy to compute and understand compact summary of topological features in various scales in a filtration. Fields where it has been successfully applied include materials science [13, 15], neuroscience [11, 14], genetics [8] and medicine [7, 18].

Over a filtration, persistence diagrams can be used because the persistence modules can be uniquely decomposed into indecomposable modules which are intervals. To these intervals, we associate the lifespans of topological features. However, when considering persistence modules over more general underlying structures, indecomposables are no longer intervals and can be more complicated.

As an example, in multidimensional persistence [6] over the commutative grid, the representation category is no longer representation finite. In other words, the number of possible indecomposables is infinite for a large enough finite commutative grid. The minimal size for a commutative grid to be representation infinite is relatively small. For two dimensional grids, we need a size of at least 2×5 or 3×3 , as the $2 \times n$ grid is representation finite for $n \leq 4$ [10]. When considering three dimensional grids, it is enough to have a $2 \times 2 \times 2$ grid. For a particular finite dimensional persistence module, it is true that it can be uniquely decomposed into a direct sum of indecomposables, but we cannot list all the possible indecomposables a priori.

From another point of view, recent progress in software [16] has made practical application of multidimensional persistence more accessible. However, they [16] approach this by computing incomplete invariants instead of indecomposable decompositions. This has the advantage of being easier to compute than the full decomposition and easier to visualize.

In this work, we aim to provide more intuition for the structure of some indecomposable modules. First, we provide algebraic constructions of some infinite families of indecomposable modules over all representation infinite grids. Next, we tackle the problem of realizing these constructions. Any module over a commutative grid can be realized as the k -th persistent homology module of a simplicial complex for any $k > 0$. This result was first claimed in [6] and proved in [12] with a construction which is straightforward algebraically but difficult to visualize. Here, we realize our infinite families of indecomposable modules using a more visual construction. In all our algebraic constructions, our infinite families depend on a dimension parameter d and a parameter $\lambda \in K$, which we set to $\lambda = 0$ for our topological constructions. Our topological constructions are formed by putting together d copies of a repeating simple pattern.

Finally we provide a Vietoris-Rips construction for our realization of the 2×5 case. Moreover, we show that this construction is stable with respect to small perturbations.

A direct corollary of our result is a constructive proof of the representation infinite type of the grids we consider. It also provides insight into one possible topological origin of these algebraic complications. Given that the construction is stable with respect to noise and appears through a relatively simple configuration, we argue that these kinds of complicated indecomposables may appear when applying multidimensional persistence to real data. Therefore these structures cannot be ignored and we hope that our construction provides insight into a source of indecomposability.

2 Background

We start with a quick overview of the necessary background. First we recall some basic definitions from the representation theory of bound quivers and detail how we check the indecomposability of representations. More details can be found in [2], for example. In the second part, we explain the block matrix formalism [1] we use to simplify some computations. We assume some familiarity with algebraic topology [17], in particular homology.

2.1 Representations of bound quivers

A quiver is a directed graph. In this work, we consider only quivers with a finite number of vertices and arrows and no cycles. A particular example is the linear quiver with n vertices. Let $n \in \mathbb{N}$ and $\tau = (\tau_1, \tau_2, \dots, \tau_{n-1})$ be a sequence of symbols $\tau_i = f$ or $\tau_i = b$. Below, the two-headed arrow \longleftrightarrow stands for either an arrow pointing to the right or left. The quiver $\mathbb{A}_n(\tau)$ is the quiver with n vertices and $n - 1$ arrows, where the i^{th} arrow points to the right if $\tau_i = f$ and to the left otherwise: $\bullet \longleftrightarrow \bullet \longleftrightarrow \dots \longleftrightarrow \bullet$. In the case that all arrows are pointing forwards, we use the notation $\vec{\mathbb{A}}_n = \mathbb{A}_n(f \dots f)$.

Throughout this work, let K be a field. A representation V of a quiver Q is a collection $V = (V_i, V_\alpha)$ where V_i is a finite dimensional K -vector space for each vertex i of Q , and each *internal map* $V_\alpha : V_i \rightarrow V_j$ is a linear map for each arrow α from i to j in Q .

A homomorphism from V to W , both representations of the same quiver Q , is a collection of linear maps $\{f_i : V_i \rightarrow W_i\}$ ranging over vertices i of Q such that $W_\alpha f_i = f_j V_\alpha$ for each arrow α from i to j . The set of all homomorphisms from V to W is the K -vector space $\text{Hom}(V, W)$. The endomorphism ring of a representation V is $\text{End}(V) = \text{Hom}(V, V)$.

General quivers do not impose any constraints on the internal maps of their representations. However, we will mostly consider the case of commutative quivers, a special kind of quiver bound by relations. In particular, representations of a commutative quiver are required to satisfy the property that they form a commutative diagram. For more details see [2]. In the rest of the article, we shall take Q to mean either a quiver or a commutative quiver, depending on context, and $\text{rep } Q$ its category of representations.

The language of representation theory was introduced to persistence in [5], where zigzag persistence modules were considered as representations of $\mathbb{A}_n(\tau)$. From now, we use the term persistence module over Q interchangeably with a representation of Q .

Any pair of representations $V = (V_i, V_\alpha)$ and $W = (W_i, W_\alpha)$ of a quiver Q has a direct sum $V \oplus W = (V_i \oplus W_i, V_\alpha \oplus W_\alpha)$ which is also a representation of Q . A representation V is said to be indecomposable if $V \cong W \oplus W'$ implies that either W or W' is the zero representation. We are concerned with the indecomposability of representations and use the following property relating the endomorphism ring with indecomposability.

Definition 1. *Let R be a ring with unity. R is said to be local if $0 \neq 1$ in R and for each $x \in R$, x or $1 - x$ is invertible.*

Lemma 1 (Corollary 4.8 of [2]). *Let V be a representation of a (bound) quiver Q .*

1. *If $\text{End } V$ is local then V is indecomposable.*
2. *If V is finite dimensional and indecomposable, then $\text{End } V$ is local.*

2.2 Block matrix formalism

Our first construction will be for a particular family of bound quivers called commutative ladders, which are the commutative grids of size $2 \times n$.

Definition 2. *The commutative ladder of length n with orientation τ , denoted $CL_n(\tau)$ is*

$$\begin{array}{ccccccc} \bullet & \longleftrightarrow & \bullet & \longleftrightarrow & \dots & \longleftrightarrow & \bullet \\ \uparrow & \circlearrowleft & \uparrow & \circlearrowleft & & \circlearrowleft & \uparrow \\ \bullet & \longleftrightarrow & \bullet & \longleftrightarrow & \dots & \longleftrightarrow & \bullet \end{array}$$

which is a quiver with two copies of $\mathbb{A}_n(\tau)$ with the same orientation τ for the top and bottom rows, and bound by all commutativity relations.

Let us review the block matrix formalism for persistence modules on commutative ladders $CL_n(\tau)$ introduced in [1]. We denote by $\text{arr}(\text{rep } \mathbb{A}_n(\tau))$ the *arrow category* (also known as the *morphism category*) of $\text{rep } \mathbb{A}_n(\tau)$, which is formed by the morphisms of $\text{rep } \mathbb{A}_n(\tau)$ as objects. The following proposition allows us to identify representations of the commutative ladder $CL_n(\tau)$ with morphisms between representations of $\mathbb{A}_n(\tau)$. Since the structure of the latter is well-understood, we use this to simplify some computations.

Lemma 2. *Let τ be an orientation of length n . There is an isomorphism of K -categories*

$$F : \text{rep } CL_n(\tau) \cong \text{arr}(\text{rep } \mathbb{A}_n(\tau)).$$

Proof. Given $M \in \text{rep } CL_n(\tau)$, the bottom row (denoted M_1) of M and the top row (denoted M_2) of M are representations of $\mathbb{A}_n(\tau)$. By the commutativity relations imposed on M , the internal maps of M pointing upwards defines a morphism $\phi : M_1 \rightarrow M_2$ in $\text{rep } \mathbb{A}_n(\tau)$. The functor F maps M to this morphism and admits an obvious inverse. \square

Each morphism $(\phi : U \rightarrow V) \in \text{arr}(\text{rep } \mathbb{A}_n(\tau))$ has representations of $\mathbb{A}_n(\tau)$ as domain and codomain. As such, Both of them can be independently decomposed into interval representations. Thus, ϕ is isomorphic to some

$$\Phi : \bigoplus_{1 \leq a \leq b \leq n} \mathbb{I}[a, b]^{m_{a,b}} \rightarrow \bigoplus_{1 \leq c \leq d \leq n} \mathbb{I}[c, d]^{m'_{c,d}}.$$

Relative to these decompositions, Φ can be written in a block matrix form $\Phi = [\Phi_{a:b}^{c:d}]$ where each block is defined by composition with the corresponding inclusion and projection

$$\Phi_{a:b}^{c:d} : \mathbb{I}[a, b]^{m_{a,b}} \xrightarrow{\iota} \bigoplus_{1 \leq a \leq b \leq n} \mathbb{I}[a, b]^{m_{a,b}} \xrightarrow{\Phi} \bigoplus_{1 \leq c \leq d \leq n} \mathbb{I}[c, d]^{m'_{c,d}} \xrightarrow{\pi} \mathbb{I}[c, d]^{m'_{c,d}}.$$

Next, we analyze these blocks by looking at the homomorphism spaces between intervals.

Definition 3. *The relation \supseteq is the relation on the set of interval representations of $\mathbb{A}_n(\tau)$, $\{\mathbb{I}[b, d] : 1 \leq b \leq d \leq n\}$, such that $\mathbb{I}[a, b] \supseteq \mathbb{I}[c, d]$ if and only if $\text{Hom}(\mathbb{I}[a, b], \mathbb{I}[c, d])$ is nonzero.*

Lemma 3 (Lemma 1 of [1]). *Let $\mathbb{I}[a, b], \mathbb{I}[c, d]$ be interval representations of $\mathbb{A}_n(\tau)$.*

1. *The dimension of $\text{Hom}(\mathbb{I}[a, b], \mathbb{I}[c, d])$ as a K -vector space is either 0 or 1.*
2. *There exists a canonical basis $\{f_{a:b}^{c:d}\}$ for each nonzero $\text{Hom}(\mathbb{I}[a, b], \mathbb{I}[c, d])$ such that*

$$(f_{a:b}^{c:d})_i = \begin{cases} 1_K : K \rightarrow K, & \text{if } i \in [a, b] \cap [c, d] \\ 0, & \text{otherwise.} \end{cases}$$

Proof. By the commutativity requirement on morphisms between representations, a nonzero morphism $g = \{g_i\} \in \text{Hom}(\mathbb{I}[a, b], \mathbb{I}[c, d])$, if it exists, is completely determined by one of its internal morphisms, $g_j \in \text{Hom}(K, K)$ for some fixed j in $[a, b] \cap [c, d]$. Since $\text{Hom}(K, K)$ is of dimension 1, part 1 follows. The $f_{a:b}^{c:d}$ in part 2 is the g determined by $g_j = 1_K$. \square

Each block $\Phi_{a:b}^{c:d} : \mathbb{I}[a, b]^{m_{a,b}} \rightarrow \mathbb{I}[c, d]^{m'_{c,d}}$ can be written in a matrix form where each entry is a morphism in $\text{Hom}(\mathbb{I}[a, b], \mathbb{I}[c, d])$. Lemma 3 allows us to factor the common basis element of each entry and rewrite $\Phi_{a:b}^{c:d}$ using a K -matrix $M_{a:b}^{c:d}$ of size $m'_{c,d} \times m_{a,b}$:

$$\Phi_{a:b}^{c:d} = \begin{cases} M_{a:b}^{c:d} f_{a:b}^{c:d}, & \text{if } \mathbb{I}[a, b] \supseteq \mathbb{I}[c, d], \\ 0, & \text{otherwise} \end{cases}$$

3 Commutative grid 2×5

We now study the construction of a family of indecomposable persistence modules for the commutative ladders of length 5. Details are provided for $\text{rep}CL_5(ffff)$ using the formalism introduced for $\text{arr}(\text{rep}\vec{\mathbb{A}}_5)$. Slight adaptations to the construction make it work for any orientation τ .

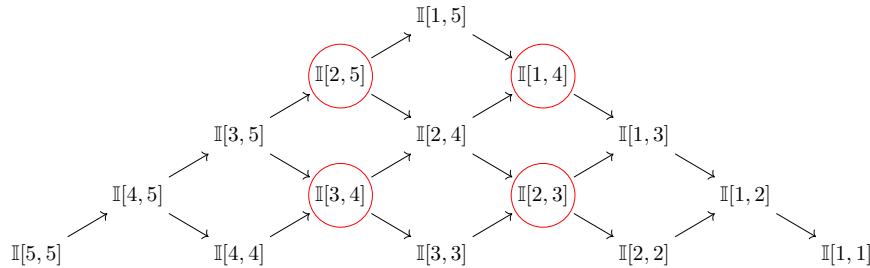
3.1 Algebraic construction

Define the interval representations $D_1 = \mathbb{I}[2, 5]$, $D_2 = \mathbb{I}[3, 4]$, $R_1 = \mathbb{I}[1, 4]$, and $R_2 = \mathbb{I}[2, 3]$ of $\vec{\mathbb{A}}_5$. Note that for each of the four choices of ordered pairs (D_i, R_j) , there exists a nonzero morphism $D_i \rightarrow R_j$, while no nonzero morphism exists between D_1 and D_2 , and between R_1 and R_2 . The directed graph with vertices given by the chosen intervals and arcs $x \rightarrow y$ defined by $x \supseteq y$ is the complete bipartite directed graph $\vec{K}_{2,2}$.

$$\begin{array}{ccc} D_1 = \mathbb{I}[2, 5] & \xrightarrow{f_{2:5}^{1:4}} & \mathbb{I}[1, 4] = R_1 \\ & \searrow^{f_{2:5}^{2:3}} & \nearrow^{f_{3:4}^{1:4}} \\ D_2 = \mathbb{I}[3, 4] & \xrightarrow{f_{3:4}^{2:3}} & \mathbb{I}[2, 3] = R_2 \end{array}$$

We provide some insight concerning this configuration from the Auslander-Reiten quiver, which describes irreducible maps between indecomposables. For our purpose, we use directed paths in the Auslander-Reiten quiver to *suggest* possible locations of nonzero maps between indecomposable representations. For $I_1 \not\cong I_2$ indecomposable representations, the presence of a directed path in the Auslander-Reiten quiver from I_1 to I_2 does *not* imply that there is a nonzero morphism $f : I_1 \rightarrow I_2$. See for example the path $\mathbb{I}[4, 4] \rightarrow \mathbb{I}[3, 4] \rightarrow \mathbb{I}[3, 3]$ below. The converse (existence of nonzero map implies directed path) does hold in the representation finite case (see Corollary IV.5.6 of [2]).

Below, we exhibit the Auslander-Reiten quiver



of $\vec{\mathbb{A}}_5$, together with our choice of indecomposables encircled.

On the other hand, for example, we note that $D'_1 = \mathbb{I}[3, 5]$, $D'_2 = \mathbb{I}[4, 4]$, $R'_1 = \mathbb{I}[2, 4]$, and $R'_2 = \mathbb{I}[3, 3]$ does not work since there is no nonzero map from D'_2 to R'_2 , even though there is a directed path from D'_2 to R'_2 in the Auslander-Reiten quiver.

Such a configuration is crucial to ensure that all four blocks can be nonzero in $\phi(d, \lambda)$ defined below, and to ensure indecomposability. The second ingredient we use is the Jordan cell $J_d(\lambda)$. Given $d \geq 1$ and $\lambda \in K$, $J_d(\lambda)$ is the matrix with value λ on the diagonal, 1 on the superdiagonal, and 0 elsewhere.

$$J_3(\lambda) = \begin{bmatrix} \lambda & 1 & 0 \\ 0 & \lambda & 1 \\ 0 & 0 & \lambda \end{bmatrix}.$$

With this, we are ready to define an arrow $\phi(d, \lambda)$ and a representation $M(d, \lambda)$, which are identified using Proposition 2 as $F(M(d, \lambda)) = \phi(d, \lambda)$.

Definition 4. Let $d \geq 1$ and $\lambda \in K$.

1. We define the arrow $\phi(d, \lambda) \in \text{arr}(\text{rep}\vec{\mathbb{A}}_5)$ $\phi(d, \lambda) : \mathbb{I}[3, 4]^d \oplus \mathbb{I}[2, 5]^d \rightarrow \mathbb{I}[1, 4]^d \oplus \mathbb{I}[2, 3]^d$ by the matrix form $\phi(d, \lambda) = \begin{bmatrix} If_{3:4}^{1:4} & If_{2:5}^{1:4} \\ If_{3:4}^{2:3} & J_d(\lambda)f_{2:5}^{2:3} \end{bmatrix}$ where I is the $d \times d$ identity matrix.

2. We also define the representation $M(d, \lambda) \in \text{rep } CL_5(ffff)$ by

$$M(d, \lambda) : \begin{array}{ccccccc} K^d & \xrightarrow{\begin{bmatrix} I \\ 0 \end{bmatrix}} & K^{2d} & \xrightarrow{\text{id}} & K^{2d} & \xrightarrow{\begin{bmatrix} I & 0 \end{bmatrix}} & K^d & \longrightarrow & 0 \\ \uparrow & & \uparrow & & \uparrow & & \uparrow & & \uparrow \\ 0 & \longrightarrow & K^d & \xrightarrow{\begin{bmatrix} I & I \\ J_d(\lambda) \end{bmatrix}} & K^{2d} & \xrightarrow{\begin{bmatrix} I & I \\ J_d(\lambda) \end{bmatrix}} & K^{2d} & \xrightarrow{\begin{bmatrix} I & I \end{bmatrix}} & K^d \\ & & & & \uparrow & & \uparrow & & \uparrow \\ & & & & 0 & & 0 & & 0 \end{array}$$

We now show that the representations constructed above are indeed indecomposable and are pairwise non-isomorphic.

Theorem 1. *Let $d \geq 1$ and $\lambda, \lambda' \in K$.*

1. $M(d, \lambda)$ is indecomposable.
2. If $\lambda \neq \lambda'$ then $M(d, \lambda) \not\cong M(d, \lambda')$.

Proof. We check that $\text{End } M(d, \lambda)$ is local. By Proposition 2, $\text{End } M(d, \lambda) \cong \text{End } \phi(d, \lambda)$. Letting (g_0, g_1) be an endomorphism of $\phi(d, \lambda)$, the diagram

$$\begin{array}{ccc} \mathbb{I}[3, 4]^d \oplus \mathbb{I}[2, 5]^d & \xrightarrow{\phi(d, \lambda)} & \mathbb{I}[1, 4]^d \oplus \mathbb{I}[2, 3]^d \\ \downarrow g_0 & & \downarrow g_1 \\ \mathbb{I}[3, 4]^d \oplus \mathbb{I}[2, 5]^d & \xrightarrow{\phi(d, \lambda)} & \mathbb{I}[1, 4]^d \oplus \mathbb{I}[2, 3]^d \end{array} \quad (1)$$

commutes. Then, g_0 and g_1 in matrix form with respect to the decompositions are

$$g_0 = \begin{bmatrix} Af_{3:4}^{3:4} & 0 \\ 0 & Bf_{2:5}^{2:5} \end{bmatrix} \text{ and } g_1 = \begin{bmatrix} Cf_{1:4}^{1:4} & 0 \\ 0 & Df_{2:3}^{2:3} \end{bmatrix}$$

where A, B, C, D are K -matrices of size $d \times d$. Since there are no nonzero morphisms from $\mathbb{I}[2, 5]$ to $\mathbb{I}[3, 4]$, nor vice versa, the off-diagonal entries of g_0 are 0. Likewise, there are no nonzero morphisms between $\mathbb{I}[1, 4]$ and $\mathbb{I}[2, 3]$ so the off-diagonal entries of g_1 are 0.

From the commutativity of Eq. (1), we get the equality

$$\begin{bmatrix} Af_{3:4}^{1:4} & Af_{2:5}^{1:4} \\ Bf_{3:4}^{2:3} & BJ_d(\lambda)f_{2:5}^{2:3} \end{bmatrix} = \begin{bmatrix} Cf_{3:4}^{1:4} & Df_{2:5}^{1:4} \\ Cf_{3:4}^{2:3} & J_d(\lambda)Df_{2:5}^{2:3} \end{bmatrix}$$

which implies that $A = B = C = D$ and $AJ_d(\lambda) = J_d(\lambda)A$ as K -matrices since the morphisms $f_{a:b}^{c:d}$ appearing above are nonzero. We infer that

$$\text{End } \phi(d, \lambda) \cong \{A \in K^{d \times d} \mid AJ_d(\lambda) = J_d(\lambda)A\}.$$

A direct computation shows that A is a member of the above ring if and only if A is upper triangular Toeplitz:

$$A = \begin{bmatrix} a_1 & a_2 & \dots & a_{d-1} & a_d \\ 0 & a_1 & a_2 & \dots & a_{d-1} \\ & & \ddots & \ddots & \vdots \\ 0 & \dots & 0 & a_1 & a_2 \\ 0 & \dots & 0 & 0 & a_1 \end{bmatrix}.$$

The matrix A is invertible if and only if a_1 is nonzero, and so for any A , either A or $I - A$ is invertible. Thus, $\text{End } \phi(d, \lambda)$ is local and $M(d, \lambda)$ is indecomposable.

By a similar computation, $M(d, \lambda) \cong M(d, \lambda')$ implies that there is some invertible matrix A such that $AJ_d(\lambda) = J_d(\lambda')A$ which is impossible when $\lambda \neq \lambda'$. \square

Proposition 1 together with the observation that if $d \neq d'$ then $M(d, \lambda) \not\cong M(d', \lambda')$ provides an easy proof for the following corollary when $\tau = ffff$. Moreover, the method above can be used to produce similar examples for any orientation τ on length $n = 5$ by finding a similar configuration isomorphic to $\vec{K}_{2,2}$ from the intervals and arcs determined by \triangleright . As a result, we get a constructive proof of the following result as a corollary.

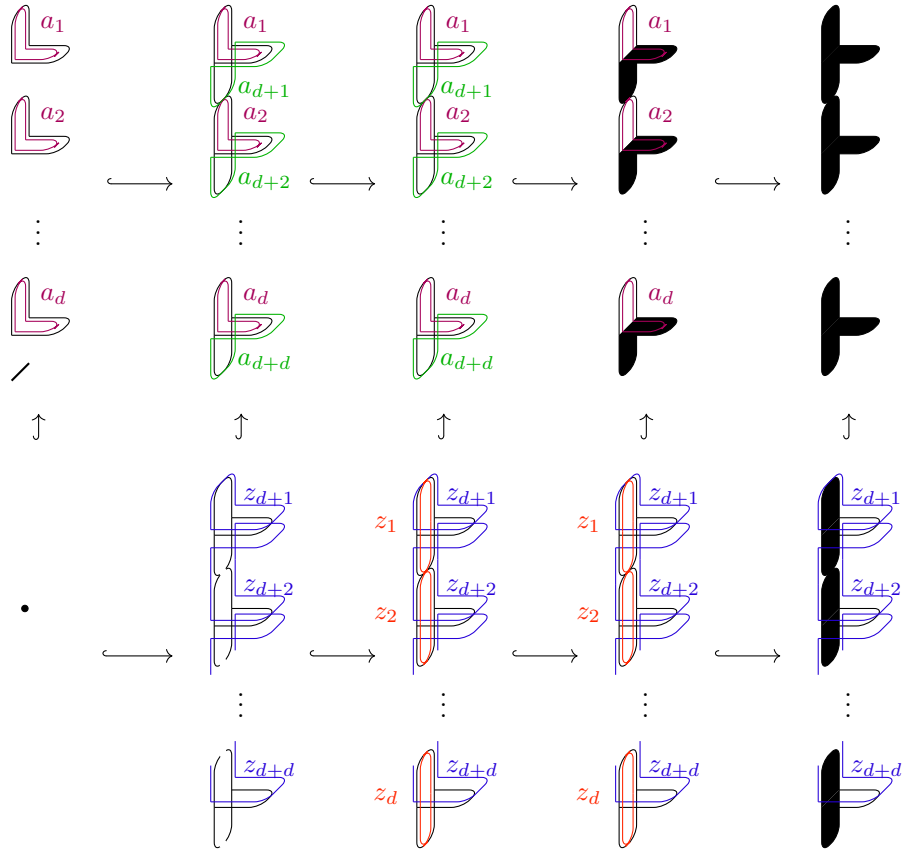
Corollary 1. For any $n \geq 5$ and orientation τ , the commutative ladder $CL_n(\tau)$ is representation infinite.

We give realizations of our indecomposable persistence modules for $\lambda = 0$, first relying purely on topological spaces and then using a geometric Vietoris-Rips construction.

3.2 Topological construction

Given $d \geq 1$, we build a diagram $\mathbb{S}(d)$ of topological spaces and inclusions. The spaces in the middle column take the form of a sandal consisting of a planar sole and a set of d straps. Other spaces are either missing some edges or have some faces filled in. Figure 1 presents the complete realization.

Figure 1: Diagram of spaces; and representatives for homology bases (in color).



The resulting diagram of spaces has maps that are all inclusions, and therefore all squares commute. Using the singular homology functor with coefficient in field K , we obtain a representation $H_1(\mathbb{S}(d))$ of $CL_5(fff)$.

Theorem 2.

$$H_1(\mathbb{S}(d)) \cong M(d, 0)$$

Proof. Relative to the choice of bases indicated in Fig. 1, the induced maps have the same matrix forms as the matrices in $M(d, 0)$. \square

3.3 Vietoris-Rips construction

Next, we use the well-known Vietoris-Rips construction to build simplicial complexes having the suitable topology. Recall that the Vietoris-Rips complex $V(P, r)$ is the clique complex of the set of all edges that

can be formed from points $p \in P$ with length less than $2r$. Note that, for $r \leq r'$, $V(P, r) \subset V(P, r')$, and hence we have a filtration.

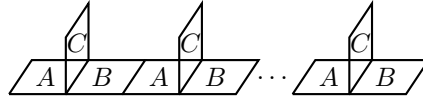
In our construction, we provide two different points sets P_ℓ and P_u corresponding to the lower and upper rows. The point sets P_ℓ and P_u are built by assembling what we call *tiles* in a regular pattern. Every tile we consider is a planar point set contained within a square with sides of length 5. We define three types of tiles: A, B, C , used for P_u and three: D, E, F , used for P_ℓ . The tile denoted \bar{E} is obtained by reflection of tile E and we call it the reversed E tile. In local coordinates, the points in the tiles are displayed in Table 1.

Table 1: Local coordinates of points within tiles.

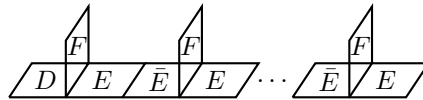
Index \ Tile	A	B	C	D	E	F	\bar{E}
1	(0, 0)	(0, 0)	(0, 0)	(0, 0)	(0, 0)	(0, 0)	(0,0)
2	(0, 5)	(0, 5)	(0, 5)	(0, 5)	(0, 5)	(0, 5)	(0,5)
3	(5, 5)	(5, 5)	(5, 5)	(5, 5)	(5, 5)	(5, 5)	(5,5)
4	(5, 0)	(5, 0)	(5, 0)	(5, 0)	(5, 0)	(5, 0)	(5,0)
5	(1.5, 0)	(1.3, 0)	(.7, 0)	(1.3, 0)	(1.3, 0)	(.5, 0)	(1.3,0)
6	(3.5, 0)	(3.7, 0)	(4.3, 0)	(3.7, 0)	(3.7, 0)	(4.5, 0)	(3.7,0)
7	(1.5, 5)	(1.3, 5)	(1.5, 5)	(1.3, 5)	(1.3, 5)	(.7, 5)	(1.3,5)
8	(3.5, 5)	(3.7, 5)	(3.5, 5)	(3.7, 5)	(3.7, 5)	(4.3, 5)	(3.7,5)
9	(0, 1.5)	(0, 0.7)	(0, 1.5)	(0, 1.3)	(0, .5)	(0, 1.3)	(0,1)
10	(0, 3.5)	(0, 4.3)	(0, 3.5)	(0, 3.7)	(0, 4.5)	(0, 3.7)	(0,4)
11	(5, 0.7)	(5, 1.5)	(5, 1.5)	(5, .5)	(5, 1)	(5, 1.3)	(5,.5)
12	(5, 4.3)	(5, 3.5)	(5, 3.5)	(5, 4.5)	(5, 4)	(5, 3.7)	(5,4.5)
13	(1.86, 2.5)	(3, 2.5)	(2.5, 2.9)	(2, 2.5)	(3, 2.5)	(2.5, 3.5)	(2,2.5)

These tiles are arranged as in Fig. 2 to obtain P_u and P_ℓ , via the union (sharing coinciding points along the shared edges) of translations of the tiles A, B, D, E, \bar{E} , and 90° rotation and translations of tiles C and F . Note that the lower row presents an asymmetry as the D tile is only used once.

Figure 2: Pattern for assembling of the tiles.



(a) For upper row P_u



(b) For lower row P_ℓ

Each tile has 13 points: one at each corner, two on the interior of each edge, and one in the interior of the tile. Via the index in Table 1, we have one-to-one correspondences between points of all tiles. We define a vertex map $f : P_\ell \rightarrow P_u$ via this correspondence, as follows. Each point $p \in P_\ell$ is a point in a copy of tile D, E, \bar{E} , or F , as in Fig. 2. Then, p is mapped to $f(p) \in P_u$ defined to be the corresponding point with the same index in Table 1 in the corresponding copy of tile A, B , or C . Note that along shared edges, there may be ambiguities as to which tile D, E, \bar{E} , or F a point $p \in P_\ell$ is coming from. However, it can be checked that the corresponding point $f(p)$ is well-defined.

We then choose five radius parameters r_1, \dots, r_5 so that $x_i < r_i < y_i$ for each i , with the bounds (x_i, y_i) described in Table 2. The values of x_i and y_i are chosen such that for all $x_i < r, r' < y_i$, $V(P_u, r) = V(P_u, r')$ and $V(P_\ell, r) = V(P_\ell, r')$.

Table 2: Ranges for the choice of parameters.

Parameter	r_1	r_2	r_3	r_4	r_5
x_i	1.06	1.21	1.6	1.8	2
y_i	1.12	1.25	1.665	1.805	2.015

We construct the diagram

$$\begin{array}{ccccccccc}
 V(P_u, r_1) & \longrightarrow & V(P_u, r_2) & \longrightarrow & V(P_u, r_3) & \longrightarrow & V(P_u, r_4) & \longrightarrow & V(P_u, r_5) \\
 f_1 \uparrow & & f_2 \uparrow & & f_3 \uparrow & & f_4 \uparrow & & f_5 \uparrow \\
 V(P_\ell, r_1) & \longrightarrow & V(P_\ell, r_2) & \longrightarrow & V(P_\ell, r_3) & \longrightarrow & V(P_\ell, r_4) & \longrightarrow & V(P_\ell, r_5)
 \end{array} \tag{2}$$

where it can be checked that for $i = 1, 2, 3, 4, 5$, the vertex map f restricted to the vertices in $V(P_\ell, r_i)$, defines a simplicial map $f_i : V(P_\ell, r_i) \rightarrow V(P_u, r_i)$. After identification of corresponding vertices by f , these are subcomplex inclusions (of abstract simplicial complexes). We note that the fact that we have subcomplex inclusions is only valid for those chosen radii, and not across the whole range of possible radii. Then, Diagram 2 has the same homology as $\mathbb{S}(d)$

Below, we provide illustrations of the Vietoris-Rips complexes restricted to the tiles, for the chosen radii.

Figure 3: Tile A

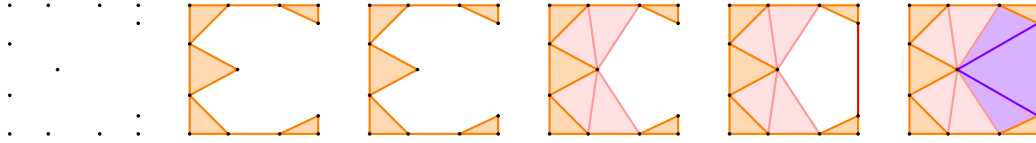


Figure 4: Tile B

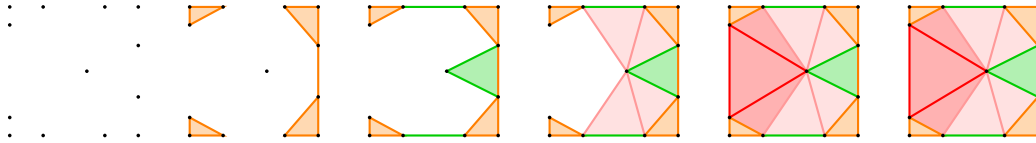


Figure 5: Tile C

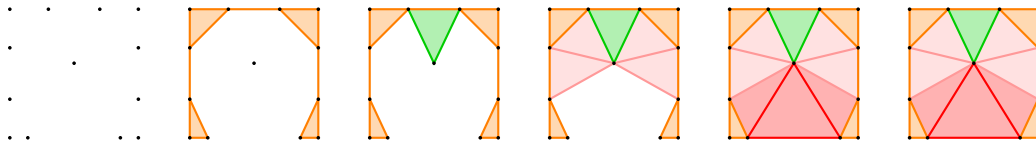


Figure 6: Tile D

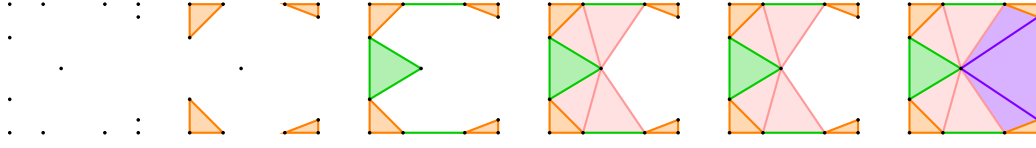


Figure 7: Tile E

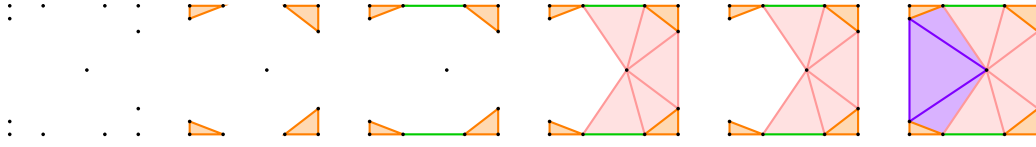


Figure 8: Tile E reversed

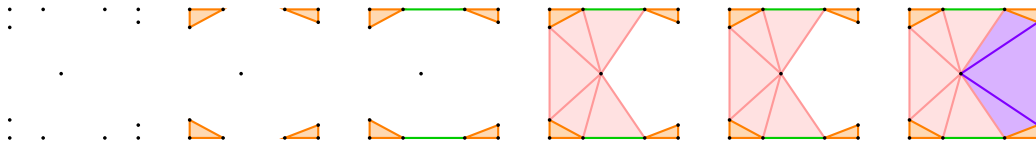
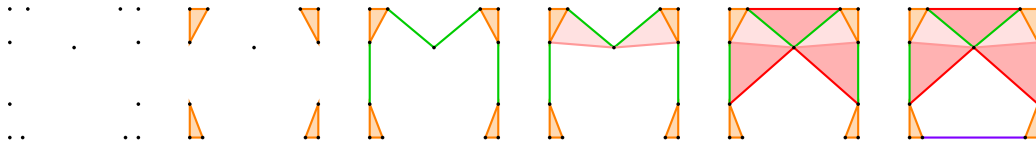


Figure 9: Tile F



The resulting Diagram 2 with $d = 2$ is displayed in Figure 10. For clarity of the illustration, we omit some extra edges and triangles that do not affect the homology.

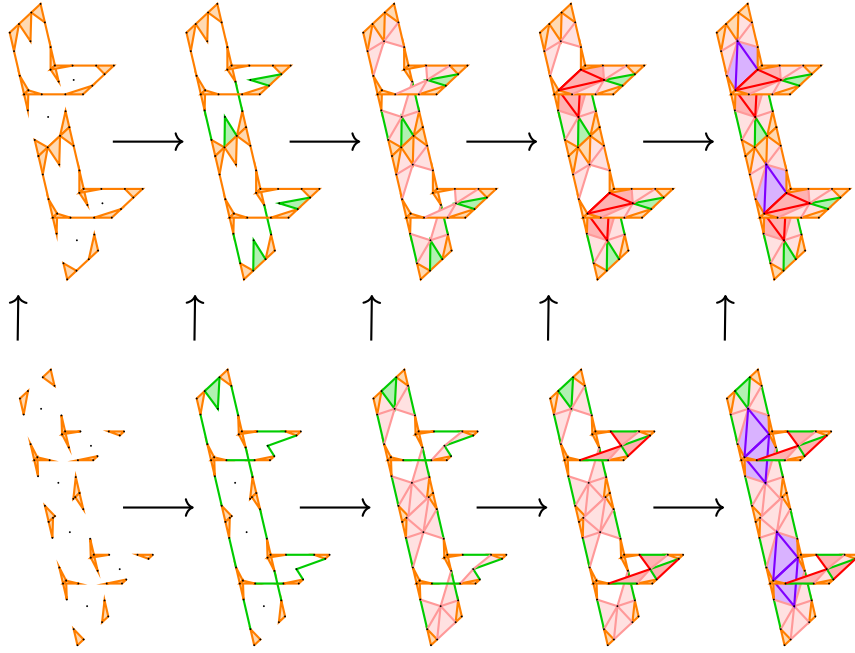
Importantly, our construction does not rely on degeneracy. With P_ℓ and P_u fixed, we can freely choose the radius parameters r_i within intervals $I_i = (x_i, y_i)$ of non-zero width where there are no changes in the filtration. Dually, small perturbations of the point sets do not change the homology of the construction. Formally we have,

Lemma 4. *Let ρ be the minimum of the diameters of I_i , and fix each r_i to be the center of I_i , for $i = 1, \dots, 5$. Replacing each point of our input by a point within a ball of radius $\frac{\rho}{2}$ around it does not change the topology.*

Proof. By construction, for any i , there are no edges of length l such that $2r_i - \rho < l < 2r_i + \rho$.

We now replace every point of P by a point located within distance $\frac{\rho}{2}$. Note that the pairwise distance after this addition of noise are modified by at most ρ . Therefore, the complexes for radii r_i are unaffected as no pairwise distance can cross that threshold. \square

Figure 10: Complete realization, $d = 2$ case



4 Commutative cube

The commutative cube C is defined to be the quiver

$$\begin{array}{ccccc}
 & & 3' & \longrightarrow & 4' \\
 & \nearrow & \uparrow & & \nearrow \\
 3 & \longrightarrow & 4 & & \uparrow \\
 & \searrow & \downarrow & & \downarrow \\
 & & 1' & \longrightarrow & 2' \\
 \uparrow & & \uparrow & & \uparrow \\
 1 & \longrightarrow & 2 & &
 \end{array}$$

bound by commutativity relations. Similar to Lemma 2, it can be checked that $\text{rep } C \cong \text{arr}(\text{rep } CL_2(f))$. Thus, we write a representation of C as a morphism between representations of $CL_2(f)$ by taking the morphism from the front face to the back face.

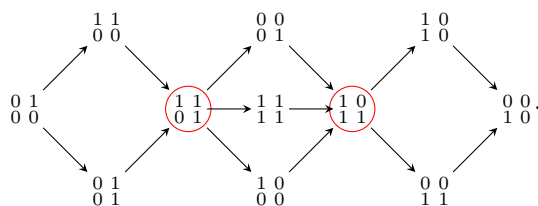
4.1 Algebraic construction

In $\text{rep}(CL_2(f))$, an analogue of Lemma 3 does not hold. In particular, the indecomposables I_1, I_2 in $\text{rep}(CL_2(f))$ given by:

$$I_1 : \begin{array}{ccc} K & \xrightarrow{1} & K \\ \uparrow & & \uparrow \\ 0 & \longrightarrow & K \end{array} \quad \text{and} \quad I_2 : \begin{array}{ccc} K & \longrightarrow & 0 \\ \uparrow & & \uparrow \\ K & \xrightarrow{1} & K \end{array}$$

have $\dim \text{Hom}(I_1, I_2) = 2$. The vector space $\text{Hom}(I_1, I_2)$ can be given the basis $\{f_2, f_3\}$, where f_2 is the identity on the lower right corner and zero elsewhere, and f_3 is the identity on the upper left corner and zero elsewhere.

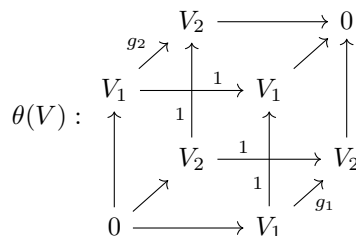
The Auslander-Reiten quiver of $CL_2(f)$, with chosen indecomposables encircled, is given by



Locating the I_1 and I_2 indecomposables and maps $f_2, f_3 : I_1 \rightarrow I_2$ employed in the construction, we see that f_2 is the composition of the morphisms on the upper path, while f_3 is of those on the lower path from I_1 to I_2 in the Auslander-Reiten quiver above.

Intuitively, we see that this is related to representations of the *Kronecker quiver* $Q_2 : 1 \rightrightarrows 2$ by thinking about the two arrows as the linearly independent f_2, f_3 . This statement can be made precise by the following.

Theorem 3. *There is a fully faithful K -functor $\theta : \text{rep } Q_2 \rightarrow \text{rep } C$ that preserves indecomposability and isomorphism classes, where θ takes a representation $V : V_1 \xrightarrow[g_2]{g_1} V_2$ to*



and a morphism $\phi = (\phi_1, \phi_2) : V \rightarrow W$ to $(0, \phi_1, \phi_1, \phi_1, \phi_2, \phi_2, \phi_2, 0) : \theta(V) \rightarrow \theta(W)$, where these maps are specified for the vertices in the order $1, \dots, 4, 1', \dots, 4'$.

Proof. That θ is a K -functor is easy to check. By the definition, $\theta(\phi) = 0$ implies that $\phi = 0$. Thus, θ is faithful. To see that θ is full, let V be as above, $W : W_1 \xrightarrow[g_2']{g_1'} W_2$ and

$$\alpha = (\alpha_1, \alpha_2, \alpha_3, \alpha_4, \alpha_{1'}, \alpha_{2'}, \alpha_{3'}, \alpha_{4'}) : \theta(V) \rightarrow \theta(W)$$

be a morphism. Then, $\alpha_1 : 0 \rightarrow 0$ and $\alpha_{4'} : 0 \rightarrow 0$ are zero maps by the forms of $\theta(V)$ and $\theta(W)$. The commutativity requirements for morphisms imply that $\alpha_2 = \alpha_3 = \alpha_4$ and $\alpha_{2'} = \alpha_{3'} = \alpha_{4'}$, and furthermore, $\alpha_{3'}g_2 = g_2'\alpha_3$ and $\alpha_{2'}g_1 = g_1'\alpha_2$. Thus, $(\alpha_2, \alpha_{2'})$ is a morphism from V to W such that $\theta((\alpha_2, \alpha_{2'})) = \alpha$.

Let $V \in \text{rep } Q_2$ be indecomposable. By part 2 of Lemma 1, $\text{End } V$ is local. By the above result that θ is fully faithful, $\text{End } \theta(V) \cong \text{End } V$, and so $\text{End } \theta(V)$ is local. Therefore, $\theta(V) \in \text{rep } C$ is indecomposable by part 1 of Lemma 1.

If $\alpha : \theta(V) \rightarrow \theta(W)$ is an isomorphism with inverse β then $(\alpha_2, \alpha_{2'}) : V \rightarrow W$ is an isomorphism with inverse $(\beta_2, \beta_{2'})$. Thus, if $\theta(V) \cong \theta(W)$, then $V \cong W$. This shows that θ preserves isomorphism classes. \square

The quiver Q_2 is representation infinite, and its indecomposable representations are well-known. See for example Proposition 1.6 of [3]. In particular, one example of an infinite family is the regular indecomposables $R_n(\lambda) : K^n \xrightarrow[J_n(\lambda)]{I} K^n$ for $n \geq 0$ and $\lambda \in K$. The following corollary is immediate from Theorem 3.

Corollary 2. *The commutative cube C is representation infinite.*

By the above arguments, $\theta(R_n(\lambda))$:

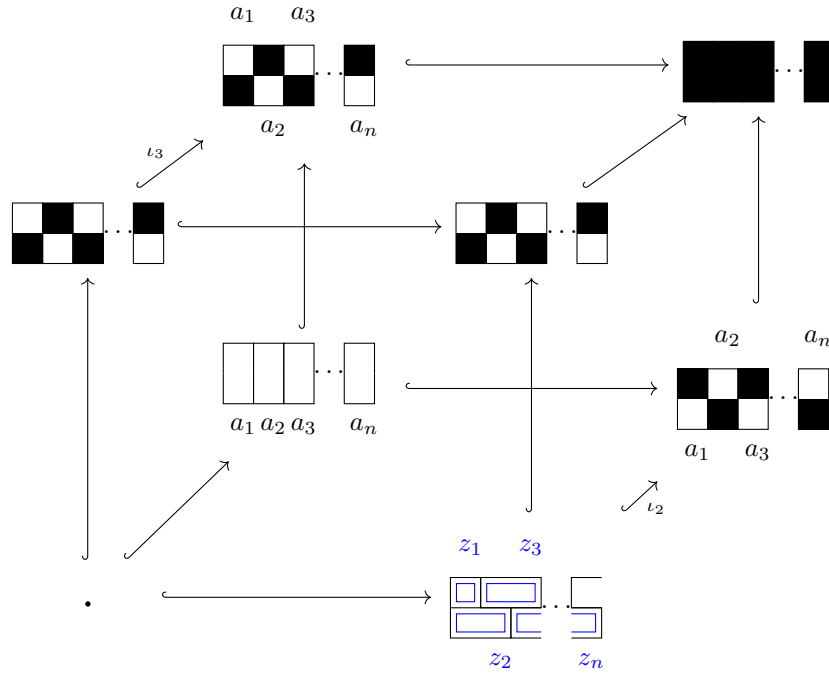
$$\theta(R_n(\lambda)) : \begin{array}{ccccc} & & K^n & \xrightarrow{\quad} & 0 \\ & \nearrow I & \uparrow & \searrow & \uparrow \\ K^n & \xrightarrow{\quad} & K^n & \xrightarrow{1} & K^n \\ & \downarrow 1 & \uparrow & \downarrow & \uparrow \\ & & K^n & \xrightarrow{1} & K^n \\ & \nearrow & \downarrow 1 & \searrow J_n(\lambda) & \uparrow \\ 0 & \xrightarrow{\quad} & K^n & \xrightarrow{\quad} & K^n \end{array}$$

are indecomposable and pairwise non-isomorphic for $n \geq 0$.

4.2 Topological construction

We give a topological realization for $\theta(R_n(0))$ in Fig. 11. In the back face, we have n half filled-in strips arranged side by side horizontally in an alternating pattern (Fig. 11 shows the case n even). Using the lower left corner, we are able to flip the pattern. Coming from the front face, and with the given choice of basis, the induced map $H_1(\iota_2)$ is $J_n(0)$ while $H_1(\iota_3)$ is the identity I .

Figure 11: Topological realization of $\theta(R_n(0))$.



5 Commutative grid 3×3

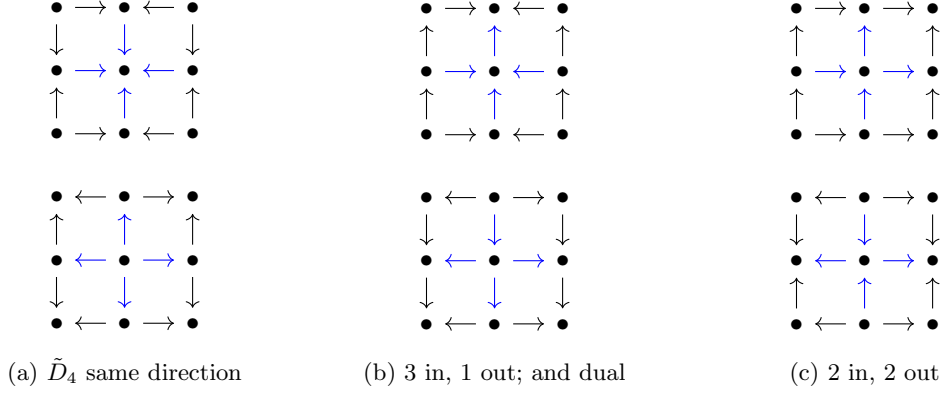
5.1 Algebraic construction

The Euclidean quiver of type \tilde{D}_4 is representation infinite for any orientation of the arrows.

$$\tilde{D}_4 : \begin{array}{ccccc} & & 1 & & \\ & & | & & \\ 2 & - & 0 & - & 4 \\ & & | & & \\ & & 3 & & \end{array}$$

We build infinite family of indecomposables for the \tilde{D}_4 -type quiver with appropriate orientation and complete it to be indecomposable representations of a 3×3 grid. Up to symmetries, there are six different orientations of the 3×3 grid. We classify them according to the resulting orientation of the central \tilde{D}_4 , shown in Fig. 12.

Figure 12: Configurations for the 3×3 grid.



We fix the vector spaces to be K^{2d} at the central vertex and K^d elsewhere. Note that at least two arrows of \tilde{D}_4 will be pointing in the same direction relative to the central vertex. On two of these arrows, we assign matrices $[I \ 0]$ and $[0 \ I]$ or $\begin{bmatrix} I \\ 0 \end{bmatrix}$ and $\begin{bmatrix} 0 \\ I \end{bmatrix}$ depending on their orientation. The remaining two arrows are assigned $[I \ J_d(\lambda)]$ or its transpose, and $[I \ I]$ or its transpose. For example, with three arrows pointing in and one out, we can have:

$$\begin{array}{c}
 K^d \\
 \uparrow [I \ J_d(\lambda)] \\
 K^d \xrightarrow{\begin{bmatrix} I \\ 0 \end{bmatrix}} K^{2d} \xleftarrow{\begin{bmatrix} I \\ I \end{bmatrix}} K^d \\
 \begin{bmatrix} 0 \\ I \end{bmatrix} \uparrow \\
 K^d
 \end{array}$$

The proof of indecomposability is again by computation of the endomorphism ring. Let $f = (f_0, \dots, f_4)$ be an endomorphism. In matrix form, $f_0 = \begin{bmatrix} A & B \\ C & D \end{bmatrix} : K^{2d} \rightarrow K^{2d}$, where 0 is the central vertex. Without loss of generality, we assume that the pair of arrows pointing in the same direction and assigned matrices $\begin{bmatrix} I \\ 0 \end{bmatrix}$ and $\begin{bmatrix} 0 \\ I \end{bmatrix}$ (or $[I \ 0]$ and $[0 \ I]$), start from (or point towards) vertices 1 and 2, respectively. From commutativity requirement for endomorphisms, $f_0 = \begin{bmatrix} A & B \\ C & D \end{bmatrix} = \begin{bmatrix} f_1 & 0 \\ 0 & f_2 \end{bmatrix}$. Suppose that the arrow assigned $[I \ I]$ (or its transpose) points to (or starts from) vertex 3. The commutativity requirement with f_3 then requires $f_1 = f_3 = f_2$. Final commutativity requirement then forces $f_1 = f_2 = f_3 = f_4$ and $f_1 J_d(\lambda) = J_d(\lambda) f_1$. Thus, the endomorphism ring is local.

Completing the example into the 3×3 grid is easy. In the squares where the representation \tilde{D}_4 provides a nonzero composition of maps, we use that composition on one arrow and the identity on the other arrow. Otherwise we simply use a 0 vector space and 0 maps.

$$\begin{array}{ccccc}
 K^d & \xrightarrow{I} & K^d & \xleftarrow{I} & K^d \\
 [I \ J_d(\lambda)] \begin{bmatrix} I \\ 0 \end{bmatrix} = I \uparrow & & \uparrow [I \ J_d(\lambda)] & & \uparrow J_d(\lambda+1) = [I \ J_d(\lambda)] \begin{bmatrix} I \\ I \end{bmatrix} \\
 K^d & \xrightarrow{\begin{bmatrix} I \\ 0 \end{bmatrix}} & K^{2d} & \xleftarrow{\begin{bmatrix} I \\ I \end{bmatrix}} & K^d \\
 \uparrow & & \begin{bmatrix} 0 \\ I \end{bmatrix} \uparrow & & \uparrow \\
 0 & \longrightarrow & K^d & \longleftarrow & 0
 \end{array}$$

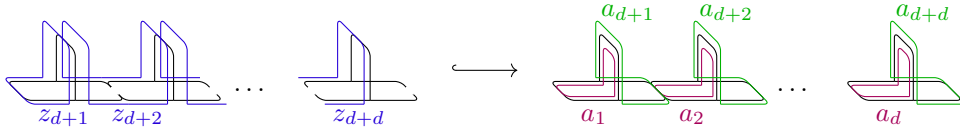
This algebraic construction can then be realized through a diagram of topological spaces and inclusions using our previous *sandal* construction. We do this in the next subsection.

5.2 Topological Construction

This subsection is split into two parts. First, we tackle the case where we have at least one arrow pointing towards the central vertex. Then we solve the remaining case where all arrows are outbound.

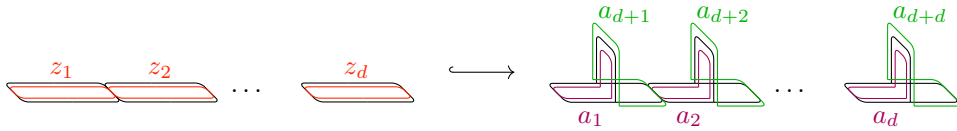
5.2.1 At least one inbound arrow

The space at the central vertex is K^{2d} . We realize it using our sandal with d straps and the basis used in Figure 1 (second space in the top row). As we have at least one arrow pointing to this space, we use again the structure from the second column of Figure 1. We end up with the following inclusion map

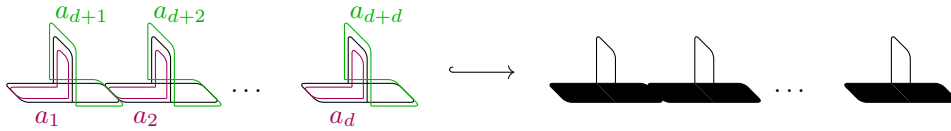


whose induced homology map is $[J_d^I(0)]$ with the indicated choice of bases.

We continue the construction by adding the matrix containing two I blocks. If the corresponding arrow points into the central vertex, we use the following inclusion, where we start with the soles without the straps:



with induced map $[I I]$. With an outbound arrow, we fill in the sole of the sandal:

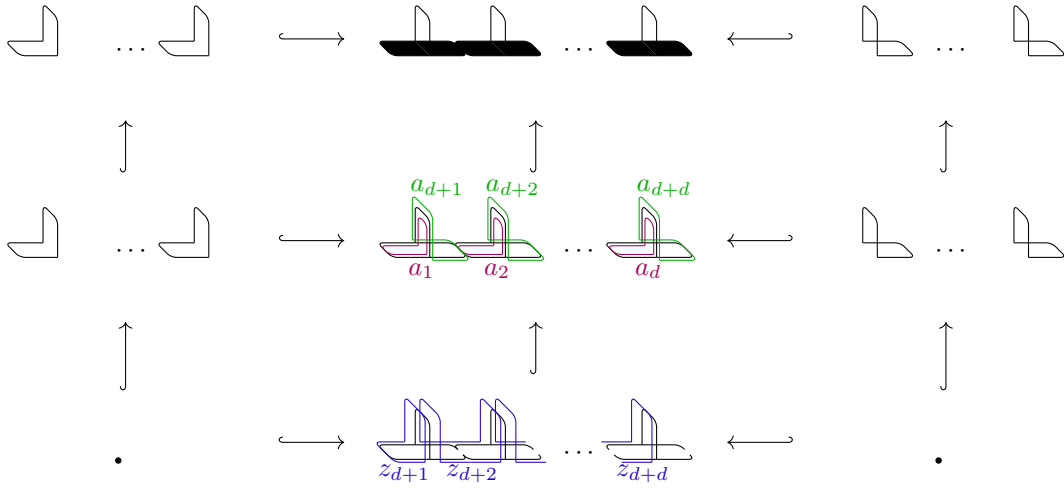


with induced map $[I I]$.

In order to complete our construction, we add simple inclusion maps as needed, maintaining as many identity maps as possible. This provide us with the following diagrams for the five possible cases. First we give the diagram of the topological spaces together with representatives for the homology bases. Second, we also provide the induced indecomposable persistence module, obtained by applying $H_1(\cdot)$.

In what follows, we list up all of the topological realizations, up to rotation of diagram. To save space, we draw only copy number 1 and d of the sandal piece (and put “...” in between) for the entries in the 3×3 grid where the topological space and choice of basis is the obvious one. Otherwise, we proceed with our usual illustration of pieces 1, 2 and d .

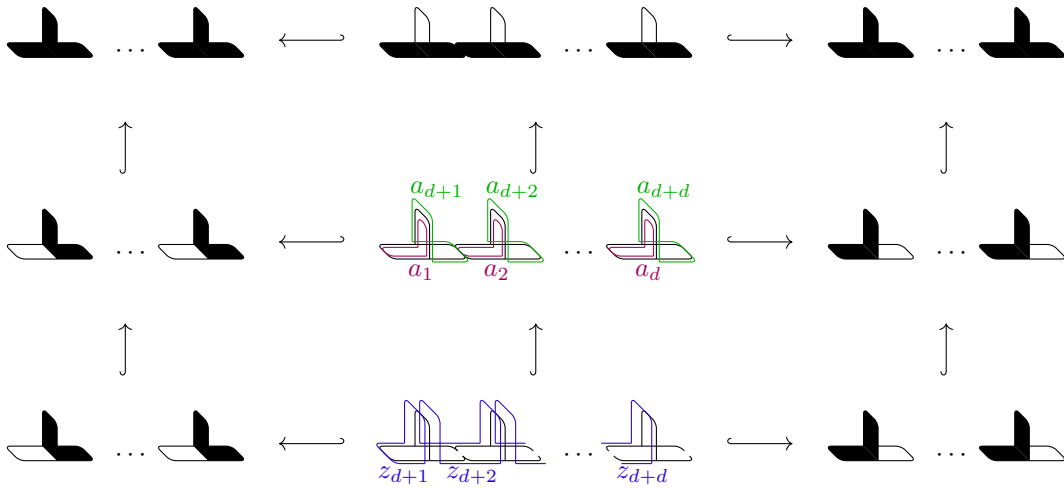
3 In 1 Out With three inbound and one outbound arrows to the central vertex, the diagram:



realizes

$$\begin{array}{ccccc}
 K^d & \xrightarrow{I} & K^d & \xleftarrow{I} & K^d \\
 I \uparrow & & \uparrow [I \ I] & & \uparrow I \\
 K^d & \xrightarrow{[I \ 0]} & K^{2d} & \xleftarrow{[0 \ I]} & K^d \\
 \uparrow [J_d(0)] & & \uparrow & & \uparrow \\
 0 & \longrightarrow & K^d & \longleftarrow & 0
 \end{array}$$

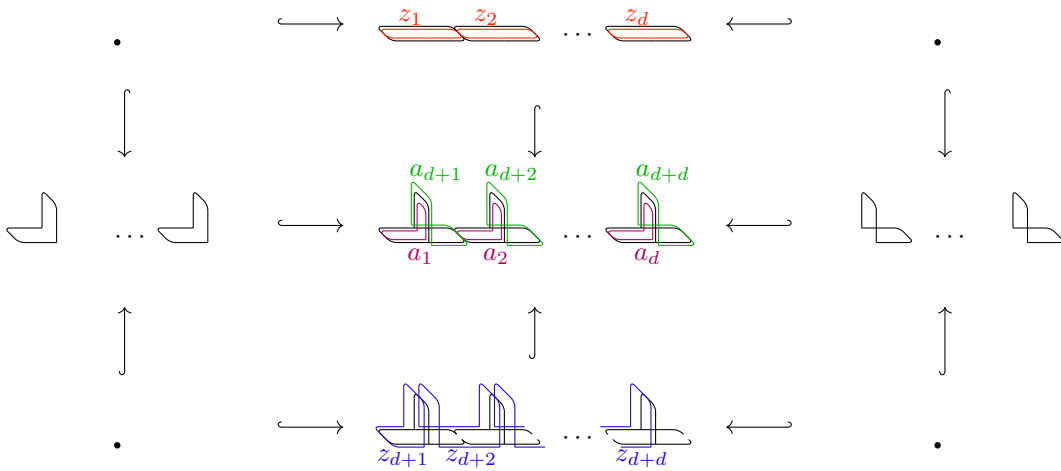
1 In 3 Out Next, with one inbound and three outbound arrows, we have the diagram:



realizing the persistence module

$$\begin{array}{ccccc}
 0 & \longleftarrow & K^d & \longrightarrow & 0 \\
 \uparrow & & \uparrow [I \ I] & & \uparrow \\
 K^d & \xleftarrow{[I \ 0]} & K^{2d} & \xrightarrow{[0 \ I]} & K^d \\
 I \uparrow & & [J_a^I] \uparrow & & I \uparrow \\
 K^d & \xleftarrow{I} & K^d & \xrightarrow{J_a(0)} & K^d
 \end{array}$$

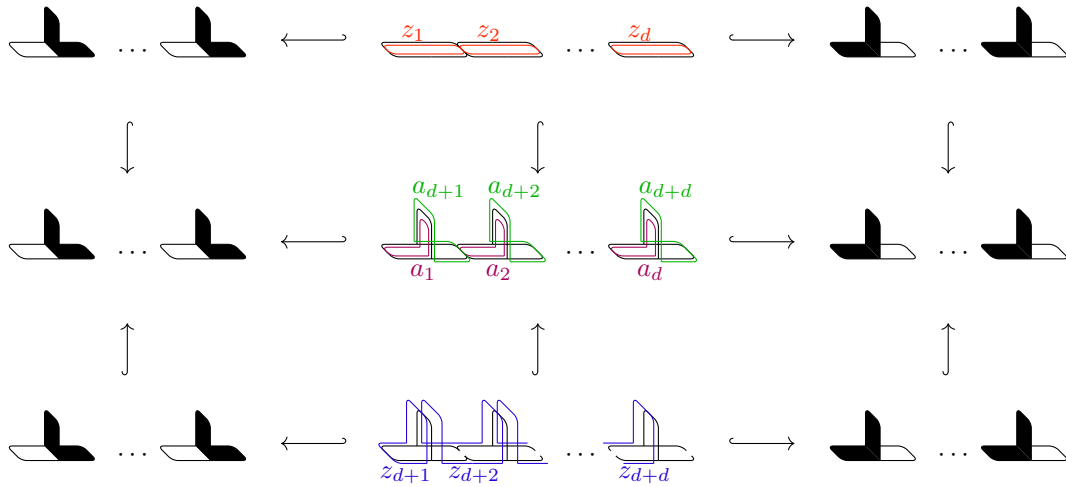
4 In With four inbound:



for the persistence module:

$$\begin{array}{ccccc}
 0 & \longrightarrow & K^d & \longleftarrow & 0 \\
 \downarrow & & \downarrow [I \ I] & & \downarrow \\
 K^d & \xrightarrow{[I \ 0]} & K^{2d} & \xleftarrow{[0 \ I]} & K^d \\
 \uparrow & & [J_a^I] \uparrow & & \uparrow \\
 0 & \longrightarrow & K^d & \longleftarrow & 0
 \end{array}$$

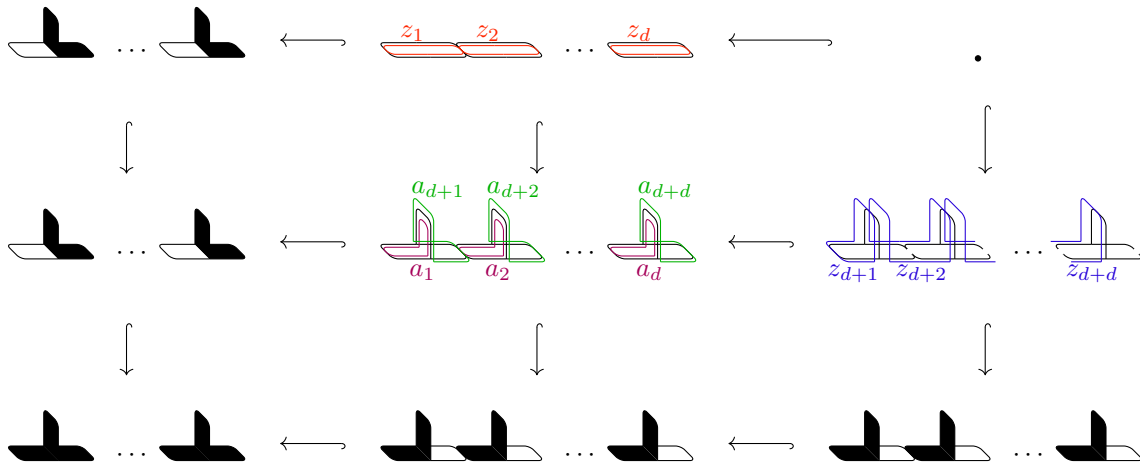
2 In 2 Out, version 1 Two inbound and two outbound, first type:



realizes

$$\begin{array}{ccccc}
 K^d & \xleftarrow{I} & K^d & \xrightarrow{I} & K^d \\
 \downarrow I & & \downarrow [I] & & \downarrow I \\
 K^d & \xleftarrow{[I \ 0]} & K^{2d} & \xrightarrow{[0 \ I]} & K^d \\
 I \uparrow & & [J_a(0)] \uparrow & & I \uparrow \\
 K^d & \xleftarrow{I} & K^d & \xrightarrow{J_a(0)} & K^d
 \end{array}$$

2 In 2 Out, version 2 Two inbound and two outbound, second type:

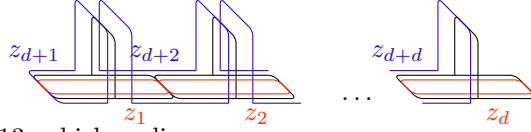


giving

$$\begin{array}{ccccc}
 K^d & \xleftarrow{I} & K^d & \xleftarrow{\quad} & 0 \\
 \downarrow I & & \downarrow [I] & & \downarrow \\
 K^d & \xleftarrow{[I \ 0]} & K^{2d} & \xleftarrow{[I]} & K^d \\
 \downarrow & & [0 \ I] \downarrow & & \downarrow J_a(0) \\
 0 & \xleftarrow{\quad} & K^d & \xleftarrow{I} & K^d
 \end{array}$$

5.2.2 No inbound arrow

For the case with no inbound arrow, we use a slightly different construction. We use the same space for the central vertex, but with a different choice of basis for homology:

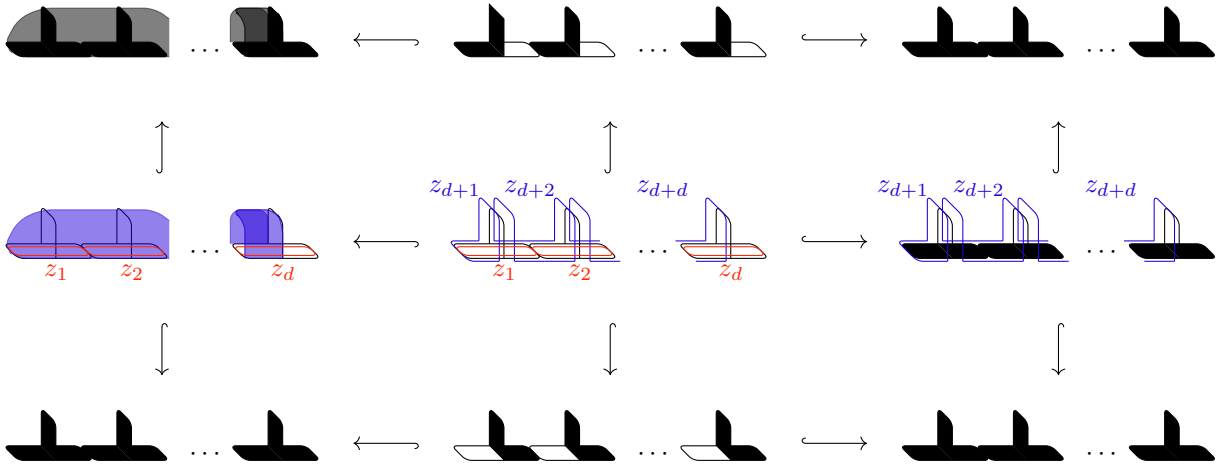


In the diagram in Figure 13, which realizes

$$\begin{array}{ccccc}
 0 & \longleftarrow & K^d & \longrightarrow & 0 \\
 \uparrow & & \uparrow [I \ J_d(0)] & & \uparrow \\
 K^d & \xleftarrow{[I \ 0]} & K^{2d} & \xrightarrow{[0 \ I]} & K^d \\
 \downarrow & & \downarrow [I \ I] & & \downarrow \\
 0 & \longleftarrow & K^d & \longrightarrow & 0
 \end{array}
 ,$$

the leftmost space on the second row is obtained by *covering* some cycles on the center so that the homology generators represented by z_{d+1}, \dots, z_{d+d} are mapped to zero, and z_1, \dots, z_d are essentially unaffected. The result is a structure that looks like a tent with no floor; or in the original analogy, it is no longer a sandal but a shoe whose sole has d holes: z_1 to z_d . Going to the space in the upper left, we simply fill these in.

Figure 13: Four arrows outbound



We thus have a topological realization for all variants of the 3×3 grid.

6 Discussion

We have illustrated constructions of infinite families of indecomposable persistence modules together with topological realizations over the small commutative grids. By embedding, this provides constructions for all possible representation infinite commutative grids.

In addition to our families of indecomposables, other parametrized families might be of interest. More generally, for representation tame commutative grids, could we realize parametrized families that generate all indecomposables?

Acknowledgement

A large part of this work was performed while both authors were affiliated with WPI-AIMR, Tohoku University, Sendai, Japan. E.G.E. was partially supported by JST CREST Mathematics 15656429. This is an expanded version of the extended conference abstract [4] presented in SoCG 2018 and the authors are thankful to the reviewers that helped improve its quality.

References

- [1] Hideto Asashiba, Emerson G. Escolar, Yasuaki Hiraoka, and Hiroshi Takeuchi. Matrix method for persistence modules on commutative ladders of finite type. *Japan Journal of Industrial and Applied Mathematics*, Sep 2018. doi:10.1007/s13160-018-0331-y.
- [2] Ibrahim Assem, Andrzej Skowronski, and Daniel Simson. *Elements of the Representation Theory of Associative Algebras: Volume 1: Techniques of Representation Theory*, volume 65. Cambridge University Press, 2006.
- [3] Michael Barot. *Introduction to the representation theory of algebras*. Springer, 2014.
- [4] Mickaël Buchet and Emerson G. Escolar. Realizations of Indecomposable Persistence Modules of Arbitrarily Large Dimension. In Bettina Speckmann and Csaba D. Tóth, editors, *34th International Symposium on Computational Geometry (SoCG 2018)*, volume 99 of *Leibniz International Proceedings in Informatics (LIPIcs)*, pages 15:1–15:13, Dagstuhl, Germany, 2018. Schloss Dagstuhl–Leibniz-Zentrum fuer Informatik. URL: <http://drops.dagstuhl.de/opus/volltexte/2018/8728>, doi:10.4230/LIPIcs.SocG.2018.15.
- [5] Gunnar Carlsson and Vin de Silva. Zigzag persistence. *Foundations of computational mathematics*, 10(4):367–405, 2010.
- [6] Gunnar Carlsson and Afra Zomorodian. The theory of multidimensional persistence. *Discrete & Computational Geometry*, 42(1):71–93, 2009.
- [7] Lorin Crawford, Anthea Monod, Andrew X. Chen, Sayan Mukherjee, and Raúl Rabadán. Topological summaries of tumor images improve prediction of disease free survival in glioblastoma multiforme. *arXiv preprint arXiv:1611.06818*, 2016.
- [8] Mary-Lee Dequeant, Sebastian Ahnert, Herbert Edelsbrunner, Thomas M. A. Fink, Earl F. Glynn, Gaye Hattem, Andrzej Kudlicki, Yuriy Mileyko, Jason Morton, Arcady R. Mushegian, et al. Comparison of pattern detection methods in microarray time series of the segmentation clock. *PLoS One*, 3(8):e2856, 2008.
- [9] Herbert Edelsbrunner, David Letscher, and Afra Zomorodian. Topological persistence and simplification. *Discrete Comput Geom*, 28:511–533, 2002.
- [10] Emerson G. Escolar and Yasuaki Hiraoka. Persistence modules on commutative ladders of finite type. *Discrete & Computational Geometry*, 55(1):100–157, 2016.
- [11] Chad Giusti, Eva Pastalkova, Carina Curto, and Vladimir Itskov. Clique topology reveals intrinsic geometric structure in neural correlations. *Proceedings of the National Academy of Sciences*, 112(44):13455–13460, 2015.
- [12] Heather A Harrington, Nina Otter, Hal Schenck, and Ulrike Tillmann. Stratifying multiparameter persistent homology. *arXiv preprint arXiv:1708.07390*, 2017.
- [13] Yasuaki Hiraoka, Takenobu Nakamura, Akihiko Hirata, Emerson G. Escolar, Kaname Matsue, and Yasumasa Nishiura. Hierarchical structures of amorphous solids characterized by persistent homology. *Proceedings of the National Academy of Sciences*, 113(26):7035–7040, 2016.
- [14] Lida Kanari, Paweł Dłotko, Martina Scolamiero, Ran Levi, Julian Shillcock, Kathryn Hess, and Henry Markram. A topological representation of branching neuronal morphologies. *Neuroinformatics*, pages 1–11, 2017.

- [15] Yongjin Lee, Senja D. Barthel, Paweł Dłotko, S. Mohamad Moosavi, Kathryn Hess, and Berend Smit. Quantifying similarity of pore-geometry in nanoporous materials. *Nature Communications*, 8, 2017.
- [16] Michael Lesnick and Matthew Wright. Interactive visualization of 2-d persistence modules. *arXiv preprint arXiv:1512.00180*, 2015.
- [17] James R. Munkres. *Elements of algebraic topology*, volume 2. Addison-Wesley Menlo Park, 1984.
- [18] Monica Nicolau, Arnold J. Levine, and Gunnar Carlsson. Topology based data analysis identifies a subgroup of breast cancers with a unique mutational profile and excellent survival. *Proceedings of the National Academy of Sciences*, 108(17):7265–7270, 2011.